The Astrophysical Journal, 699:L43–L47, 2009 July 1 doi:10.1088/0004-637X/699/1/L43

THE RADIO AGN POPULATION DICHOTOMY: GREEN VALLEY SEYFERTS VERSUS RED SEQUENCE LOW-EXCITATION ACTIVE GALACTIC NUCLEI

V. Smolčić
California Institute of Technology, MC 105-24, 1200 East California Boulevard, Pasadena, CA 91125, USA
Received 2009 March 19; accepted 2009 May 14; published 2009 June 15

ABSTRACT

Radio outflows of active galactic nuclei (AGNs) are invoked in cosmological models as a key feedback mechanism in the latest phases of massive galaxy formation. Recently, it has been suggested that the two major radio AGN populations—the powerful high-excitation, and the weak low-excitation radio AGNs (HERAGN and LERAGN, respectively)—represent two earlier and later stages of massive galaxy buildup. To test this, here we make use of a local ($0.04 < z < 0.1$) sample of ∼500 radio AGNs with available optical spectroscopy, drawn from the FIRST, NVSS, SDSS, and 3CRR surveys. A clear dichotomy is found between the properties of low-excitation (absorption line AGN and LINERs) and high-excitation (Seyferts) radio AGNs. The hosts of the first have the highest stellar masses, reddest optical colors, and highest mass black holes but accrete inefficiently (at low rates). On the other hand, the high-excitation radio AGNs have lower stellar masses, bluer optical colors (consistent with the "green valley"), and lower mass black holes that accrete efficiently (at high rates). Such properties can be explained if these two radio AGN populations represent different stages in the formation of massive galaxies, and thus are also linked to different phases of the "AGN feedback."

Key words: cosmology: observations – galaxies: active – galaxies: evolution – galaxies: fundamental parameters – radio continuum: galaxies

1. INTRODUCTION

Observational studies at various wavelength regimes have converged toward a widely accepted galaxy evolution picture. In this scenario, galaxies are thought to evolve in time from an initial star-formation-dominated state with blue optical colors into the most massive "red-and-dead" galaxies (Bell et al. 2004a, 2004b; Borch et al. 2006; Faber et al. 2007; Brown et al. 2007; Hopkins et al. 2007). The transitional phase, that links the blue and red galaxy states, is reflected in a sparsely populated region in color–magnitude diagrams that is referred to as the "green valley."[1] On the other hand, past cosmological models have been unsuccessful in describing the formation of massive galaxies (e.g., White & Rees 1978; White & Frenk 1991). They have led to systematic overpredictions of the number of both massive blue, and the most massive red galaxies in the universe. Only recently have these problems been overcome by implementing "AGN feedback" in the models (Croton et al. 2006; Bower et al. 2006; Hopkins et al. 2006; Sijacki & Springel 2006; Sijacki et al. 2007). Two types of AGN feedback are often invoked. The first is known as the "quasar" or "truncation" mode. In this mode quasar winds are thought to quench star formation, and cause galaxies to fade to red colors by expelling a fraction of the gas from the galaxy. The second, often referred to as "radio" or "maintenance" mode, is linked to radio AGN outflows in already massive, red galaxies. These outflows are thought to heat the surrounding medium, and thereby prevent further star formation in the galaxy and hence limit growth from creating overly high-mass galaxies. Although observational evidence supporting AGN feedback is growing (Best et al. 2006; Bundy et al. 2008; Nesvadba et al. 2008; Smolčić et al. 2009), its impact on galaxy formation and evolution is still poorly understood. Here we focus on studying the link between radio AGN activity and massive galaxy formation.

[1] Note, however, that not all galaxies in the "green valley" are necessarily transition objects.

Studies of radio AGN suggest that powerful ($L_{1.4\,\mathrm{GHz}} \gtrsim 10^{25}$ W Hz^{-1}) and weak ($L_{1.4\,\mathrm{GHz}} < 10^{25}$ W Hz^{-1}) radio AGNs represent different galaxy populations (e.g., Fanaroff & Riley 1974; Ledlow & Owen 1996; Kauffmann et al. 2008). Based on a sample of local radio AGN, Kauffmann et al. (2008) have shown that those with strong emission lines of high-ionization potential species are predominantly powerful in radio. As has been suggested in a model developed by Hardcastle et al. (2006), this high/low excitation classification may represent a principal separator between populations fundamentally different in their black hole accretion mechanisms (see also Evans et al. 2006; Allen et al. 2006; Kewley et al. 2006). In this model, central supermassive black holes of high-excitation radio AGN (HERAGN hereafter) accrete in a standard (radiatively efficient) way from the cold phase of the intragalactic medium (IGM), while those of low-excitation radio AGN (LERAGN hereafter) are powered in a radiatively inefficient manner by Bondi accretion of the hot IGM. Although still awaiting a robust confirmation, this model successfully explains many observed properties of radio AGN.

Recently, Smolčić et al. (2009) have used a unique sample of weak (VLA-COSMOS; Schinnerer et al. 2007; Smolčić et al. 2008) radio AGN, that reaches out to $z = 1.3$, to study their host galaxies, and cosmic evolution. They find that (1) already at $z \sim 1$, weak radio AGNs occur in red-sequence galaxies with the highest stellar and black hole masses, and (2) contrary to powerful radio AGNs, the volume-averaged number density of weak radio AGN evolves only modestly with cosmic time (see Smolčić et al. (2009) and references therein). Based on these results, they have proposed an evolutionary scenario in which powerful (predominantly high excitation) and weak (predominantly low excitation) radio AGNs represent different (i.e., earlier and later, respectively) stages of the blue-to-red galaxy evolution. This scenario suggests that the triggering of radio AGN activity is a strong function of host galaxy properties, linked to different stages of massive galaxy formation. It also

illuminates the mechanisms of "AGN feedback," regularly invoked in cosmological models, as it suggests that powerful and weak radio AGN activities are bound to different types of feedback.

The main goal of this Letter is to test the above outlined models and scenarios. To do this we utilize a large local sample of radio AGN (Section 2), in which accurate low/high excitation classifications can be obtained. In Section 3, we explore the fundamental differences between these types of radio AGNs, and we put them into a perspective of massive galaxy buildup in Section 4.

2. THE FIRST–NVSS–SDSS RADIO AGN SAMPLE

In order to investigate the principal differences between various radio AGN types, we make use of a unified catalog of radio objects detected by NVSS, FIRST, WENSS, GB6, and SDSS (Kimball & Ivezić 2008). We have augmented this catalog with derivations of emission-line fluxes, 4000 Å breaks, stellar masses, and stellar velocity dispersions, drawn from the SDSS-DR4 "main" spectroscopic sample (see Kauffmann et al. 2003a, 2003b and reference therein).[2] The cross-correlation yielded 20,648 radio object entries in the catalog with available line flux measurements.[3] Following Kimball & Ivezić (2008), we further limit this catalog to 6640 unique objects that have been detected by both the FIRST and NVSS surveys at 20 cm (equivalent to sample "C" in their Table 8, but without the "overlap = 1" criterion).

In order to access the most accurate emission-line flux estimates, we restrict the above-defined sample of unique objects in redshift to $0.04 < z < 0.1$, and select only sources with stellar mass, and 4000 Å break measures.[4] We define emission-line galaxies as those where the relevant emission lines (Hα, Hβ, O[III,λ5007], N[II,λ6584]) have been detected at signal-to-noise ratio (S/N) $\geqslant 3$, and consider all galaxies with S/N < 3 in these lines as absorption line systems. Given that the latter are luminous at 20 cm, they can be considered to be (low-excitation) AGNs (see, e.g., Best et al. 2005; Smolčić et al. 2008 for a more detailed discussion). Further, using standard optical spectroscopic diagnostics (Baldwin et al. 1981; Kauffmann et al. 2003b; Kewley et al. 2001, 2006), we sort the emission-line galaxies into (1) star-forming, (2) composite, (3) Seyfert, and (4) LINER galaxies (see Figure 1). The last two classes have been selected by requiring S/N $\geqslant 3$ in S[II,$\lambda\lambda$6717,6731] and [O I, λ6300], as well as "unambiguously" by imposing combined criteria using three emission-line flux ratios (see the middle and right panels in Figure 1).

The spectroscopic selection yields final samples of $\sim$310 star-forming galaxies and $\sim$480 AGNs, out of which $\sim$110 are "unambiguous" Seyferts, $\sim$120 are "unambiguous" LINERs, and $\sim$250 are absorption line systems. Hereafter, we will separately analyze the properties of absorption line AGNs, LINERs, and Seyferts, keeping in mind that the first two are low-excitation systems, while the last has luminous and hard UV sources which ionize the observed emission lines (e.g., Kewley et al. 2006). The full range of 20 cm radio power[5] in these samples is $\sim 10^{22}$–10^{25} W Hz^{-1}.

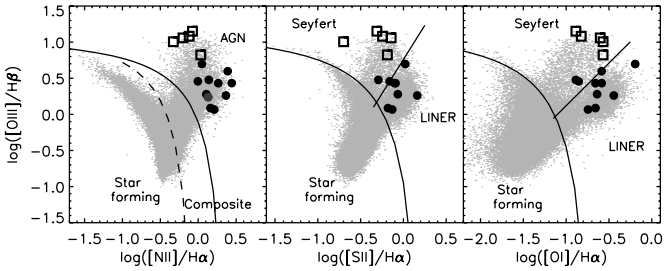

Figure 1. Optical spectroscopic diagnostic diagrams (see Kauffmann et al. 2003b; Kewley et al. 2006) that separate emission-line galaxies into star-forming, composite galaxies, and various types of AGNs (Seyferts and LINERs). Small gray dots represent galaxies from the SDSS DR4 "main" spectroscopic sample. Large open squares (filled dots) denote $z < 0.1$ 3CRR radio galaxies independently classified (based on their core X-ray emission) as systems with radiatively efficient (inefficient) black hole accretion (Evans et al. 2006).

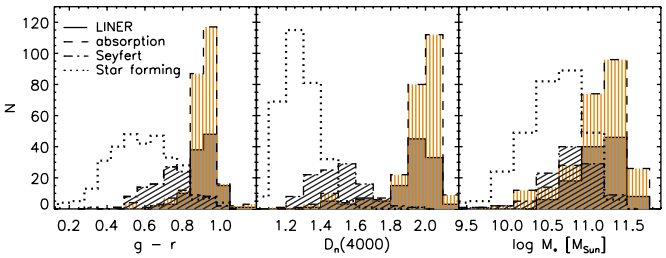

Figure 2. Distribution of $g-r$ (left), 4000 Å break (middle), and logarithm of stellar mass (right) for radio luminous LINERs (filled histograms), absorption line systems (vertically hatched histograms), and Seyferts (diagonally hatched histograms), drawn from the FIRST–NVSS–SDSS sample. For comparison, the distribution of radio luminous star-forming galaxies is also shown. Note that Seyfert, i.e., high-excitation, radio sources occupy an intermediate region between star-forming and low-excitation (LINERs and absorption line) AGNs in these diagrams.

3. RADIO AGN HOST GALAXY PROPERTIES

In Figure 2, we show the distributions of color, 4000 Å break strength [$D_n(4000)$], and stellar mass for the host galaxies of radio luminous AGN, spectroscopically divided into Seyfert, LINER, and absorption line galaxies. While LINER and absorption line systems follow very similar distributions (as expected if low-excitation systems form one family), there are obvious differences compared to Seyfert galaxies. The former on average have redder optical $g-r$ colors (left panel in Figure 2), larger values of $D_n(4000)$ (implying older stellar populations; middle panel), and higher stellar masses (left panel). From these plots, it is obvious that Seyfert galaxies represent a population with properties in an intermediate range, linking those of star-forming galaxies at one extreme to those of massive red galaxies at the other. In particular, Seyfert galaxies in the FIRST–NVSS–SDSS sample are consistent with "green valley" objects, a population thought to be in transition from star-formation-dominated—to a "red-and-dead"—state (e.g., Faber et al. 2007). We will discuss this further in Section 4.

In order to investigate the central supermassive black hole properties of radio AGNs, in Figure 3 we show the distribution of stellar velocity dispersion (σ), and the ratio of O[III] luminosity and σ^4 for the LINERs and Seyferts in the FIRST–NVSS–SDSS sample. As black hole mass is tightly correlated with

[2] The catalogs with emission-line fluxes (emission_lines_v5.0_4.fit), and stellar mass, $D_n(4000)$, and stellar velocity dispersions (agn.dat_dr4_release.v2) have been downloaded from www.mpa-garching.mpg.de/SDSS/DR4/

[3] This catalog is available at www.astro.caltech.edu/~vs/RadioCat.php

[4] This includes all galaxies with available stellar velocity dispersion, and O[III] luminosity estimates.

[5] Computed using the NVSS total flux densities (F_ν), and assuming a spectral index of $\alpha = 0.7$ ($F_\nu \propto \nu^{-\alpha}$).

Table 1
Properties of 3CRR Radio AGN

Name	Redshift	N[II]/Hα	S[II]/Hα	O[I]/Hα	O[III]/Hβ	log $M_{\rm BH}$	$L_{0.5-10{\rm keV}}/L_{\rm EDD}$
3C 33	0.060	0.630	0.720	0.250	11.452	8.68	1.6×10^{-03}
3C 98	0.030	0.760	0.570	0.150	12.040	8.23	3.7×10^{-04}
3C 390.3	0.056	0.470	0.200	0.270	10.125	8.53	1.1×10^{-02}
3C 403	0.059	0.840	0.490	0.130	14.160	8.41	3.3×10^{-03}
3C 452	0.081	1.080	0.650	0.270	6.652	8.54	3.3×10^{-03}
3C 31	0.017	0.990	0.690	0.140	2.867	7.89	$< 2.0 \times 10^{-04}$
3C 449	0.017	1.380	0.510	0.130	3.000	7.71	$< 7.0 \times 10^{-03}$
3C 66B	0.022	2.450	...	0.260	3.955	8.84	$< 4.4 \times 10^{-05}$
3C 83.1B	0.027	1.350	...	...	1.736	9.01	$< 6.8 \times 10^{-06}$
3C 84	0.018	1.120	1.050	0.640	4.976	9.28	$< 9.2 \times 10^{-06}$
3C 264	0.022	1.450	0.660	0.220	1.222	8.85	$< 1.8 \times 10^{-05}$
3C 272.1	0.004	1.280	0.860	0.230	1.900	9.18	$< 8.5 \times 10^{-07}$
3C 274	0.004	2.320	1.450	0.360	1.824	9.38	$< 4.3 \times 10^{-07}$
3C 296	0.025	1.840	0.810	0.220	2.700	9.13	$< 1.2 \times 10^{-05}$
3C 338	0.032	1.630	0.740	0.180	1.167	9.23	$< 2.0 \times 10^{-05}$
3C 465	0.030	2.770	0.790	0.260	2.706	9.32	$< 2.2 \times 10^{-04}$

Notes.
The first column represents the 3CRR source. The second column shows the redshift, and Columns 3–6 line flux ratios for each source (shown in Figure 1 and adopted from Buttiglione et al. 2009). The last two columns, adopted from Evans et al. (2006, E06), represent the black hole mass, and accretion efficiency (in Eddington units) for each AGN (see the text for details; the upper limits are obtained assuming $N_H = 10^{24}$ atoms cm^2; see E06). Radiatively efficient (top) and inefficient (bottom) accretors, as defined by E06 based on their core X-ray emission, are separated by the double horizontal line. The single horizontal line separates Seyferts (top) and LINERs (bottom), identified here based on their optical spectroscopic properties (see Figure 1, and text for details).

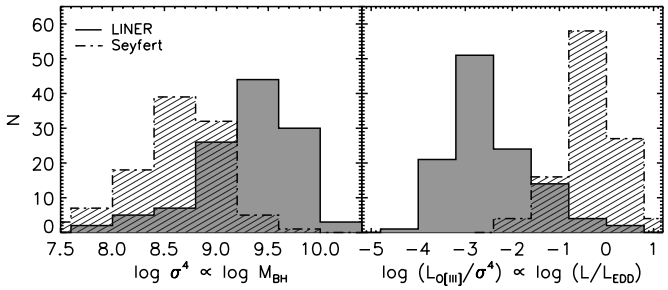

Figure 3. Distribution of (a) velocity dispersion, σ^4 (left panel), which is proportional to black hole mass (Tremaine et al. 2002), and (b) log $L_{\rm O[III]}/\sigma^4$ (right panel), proportional to black hole accretion rate (in Eddington units; Heckman et al. 2004) for radio luminous LINERs (filled histograms), and Seyferts (hatched histograms) studied here.

the bulge stellar velocity dispersion ($\log M - {\rm BH} = 8.13 + 4.02 \log \frac{\sigma}{200 {\rm km\,s^{-1}}}$; Tremaine et al. 2002), log σ is a proxy for black hole mass. Furthermore, as $L_{\rm O[III]}$ traces well the AGN bolometric luminosity (see Heckman et al. 2004 for details), the quantity $L_{\rm O[III]}/\sigma^4$ is proportional to the mass accretion rate onto the black hole (in Eddington units; $L/L_{\rm EDD} = \dot{M}_{\rm BH}/\dot{M}_{\rm EDD}$). Figure 3 shows that radio luminous LINERs have systematically higher black hole masses, and lower accretion rates (in Eddington units) than radio luminous Seyferts. This is consistent with the overall properties of LINER and Seyfert galaxies (Ho 2005; Kewley et al. 2006), and in support of the radio AGN scenario developed by Hardcastle et al. (2006), and based on the results presented in Evans et al. (2006, E06 hereafter).

Using high-resolution X-ray imaging of radio cores in a sample of 22 3CRR ($z < 0.1$) radio galaxies, E06 have studied accretion rates in various types of radio AGNs. They have found that X-ray cores of usually powerful, edge-brightened (FR II) radio galaxies are dominated by absorbed, accretion-related emission. Contrary to this, they find that X-ray cores of typically weak, core-dominated (FR I) radio galaxies likely arise from a jet, and any additional accretion-related components in these have low radiative efficiencies. Based on these results, Hardcastle et al. (2006) have assumed that it is the excitation state (rather than radio morphology) that is the principal separator of the black hole accretion mechanism in radio AGN. Recently, high-quality optical spectroscopy, that allows a robust high/low excitation classification of the E06 sample, has become available. Buttiglione et al. (2009) have computed emission-line fluxes for a large number of radio AGNs, including most of the galaxies in the E06 sample. Thus, it is now possible to view the E06 sample robustly separated into low-excitation (LINER) and high-excitation (Seyfert) state systems. In Figure 1, we have overplotted the 3CRR galaxies studied in E06 with available spectroscopic line measurements. The properties of this sample are summarized in Table 1. Figure 1 clearly shows that the 3CRR radio galaxies independently classified as radiatively inefficient accretors (E06) are LINERs, while those identified as accreting efficiently are Seyferts (see also the last column in Table 1). Only two galaxies (3C 31 and 3C 449) are classified here as Seyferts, yet they have been identified as radiatively inefficient accretors by E06. However, as evident from Table 1, their black hole accretion efficiencies may also be consistent with radiatively efficient accretion. Overall, the black hole masses of the 3CRR LINER galaxies ($\langle \log M_{\rm BH} \rangle = 9.14 \pm 0.06\ M_\odot$) are systematically higher than those of 3CRR Seyferts ($\langle \log M_{\rm BH} \rangle = 8.3 \pm 0.1\ M_\odot$), consistent with the black hole properties of FIRST–NVSS–SDSS LINERs and Seyferts.

4. SUMMARY AND DISCUSSION

We have based this study on a local ($0.04 < z < 0.1$) 20 cm selected sample of radio AGN detected by the FIRST and NVSS surveys. By cross-matching this sample with optical spectroscopic measurements from the SDSS survey, we have investigated the principal host galaxy and central supermassive black hole differences between various types of radio AGNs.

In the following, we will refer to the radio LINER and absorption line AGN as low-excitation radio AGN (LERAGN), and to Seyferts as high-excitation radio AGN (HERAGN). Furthermore, we take the powerful ($L_{1.4\,\mathrm{GHz}} \gtrsim 10^{25}$ W Hz^{-1}) and weak ($L_{1.4\,\mathrm{GHz}} < 10^{25}$ W Hz^{-1}) radio AGNs to be predominantly high- and low-excitation systems, respectively (based on the results from Section 1).

4.1. The Black Hole Properties of Radio AGNs: A Low/High Excitation State Dichotomy

Based on the FIRST–NVSS–SDSS sample we have shown that the mass accretion rates (in Eddington units) in low-excitation radio AGNs are on average substantially lower than in high-excitation radio AGNs, while the trend is opposite for their black hole masses. This is consistent with the high-resolution X-ray analysis of the cores of local 3CRR radio galaxies (E06). Combining these with recent line flux measurements (Buttiglione et al. 2009) suggests that LERAGN accrete onto their black holes in a radiatively inefficient way, while the black hole accretion in HERAGN occurs via a standard thick disk in a radiatively efficient manner. Thus, the division of radio AGNs into low- and high-excitation sources seems to be a good proxy for identifying radio AGNs, fundamentally different in their central supermassive black hole properties. Furthermore, we have shown that these two types of radio AGNs show systematic differences also in their host galaxy properties on large (kpc) scales. As outlined below, this link between pc-scale and kpc-scale galaxy properties may be explained if HE- and LE-RAGN represent different stages in the process of massive red galaxy formation.

4.2. The Low/High Excitation Radio AGN Dichotomy in the Context of Massive Galaxy Formation

Galaxies are thought to evolve in time from an initial stage with irregular or spiral morphology and blue optical colors toward elliptical morphologies with red optical colors and the highest stellar masses ($M_* \gtrsim 10^{11}\ M_\odot$; e.g., Faber et al. 2007). In the context of this red massive galaxy formation picture, the results presented here imply that LERAGN and HERAGN represent different stages of this process. As summarized in Figure 4, low-excitation radio AGNs are predominantly hosted by the most massive galaxies, with the reddest colors, consistent with final stages of massive red galaxy formation. On the other hand, the host galaxies of high-excitation radio AGNs have colors consistent with a transitional region ("green valley") between blue and red galaxies (see also Section 3). Compared to LER-AGN, they on average have younger stellar populations, lower black hole masses, and higher accretion rates (see Section 3). Such properties are consistent with an intermediate, very active phase in which galaxies are undergoing substantial stellar and black hole mass buildup on their evolutionary path toward a massive "red-and-dead" state.

Our results are in agreement with the scenario presented by Smolčić et al. (2009). Based on a study of the evolution of weak (VLA-COSMOS) and powerful (3CRR, 6CE, and 7CRS; Willott et al. 2001) radio AGNs since $z = 1.3$, they have proposed that powerful (high-excitation) radio AGNs represent an intermediate stage in the formation of a massive red galaxy, while weak (low-excitation) radio AGNs occur in the latest phases of this process when the galaxy has already assembled both its stellar and black hole masses. Thus, in the context of AGN feedback as a relevant mechanism for the formation of massive galaxies, only LERAGN, i.e., weak ($L_{1.4\,\mathrm{GHz}} < 10^{25}$ W Hz^{-1}) radio AGNs, are expected to contribute to the so-called "radio mode" feedback, responsible for limiting stellar mass growth. Namely, in cosmological models, this mode becomes important when a galaxy has already assembled most of its mass, and it has formed a hot spherical halo. Such properties are observed in massive galaxies that host predominantly *weak* radio AGNs. On the other hand, the results presented here show that HERAGN, i.e., powerful ($L_{1.4\,\mathrm{GHz}} > 10^{25}$ W Hz^{-1}) radio AGNs, occur in a "transitional" evolutionary state linking blue star-forming and massive red galaxies. Thus, in terms of AGN feedback, powerful radio AGN outflows are more closely linked to a different feedback phase, namely the "quasar mode" thought to be relevant for star formation quenching in galaxies that causes blue star-forming galaxies to fade to redder colors.

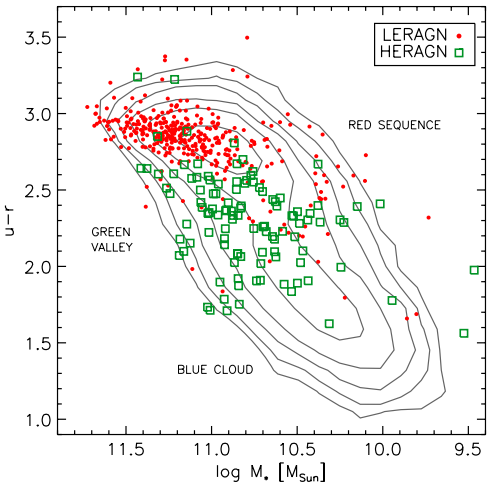

Figure 4. $u-r$ color vs. stellar mass for the general population of galaxies ($0.04 < z < 0.1$; drawn from the sample used in Smolčić et al. 2006) shown in contours. The contour levels start at 26, and continue in steps of 2^n ($n = 1, 2, \ldots, 5$). The distributions of low- and high-excitation radio AGNs (LERAGN and HERAGN, respectively) are also shown (filled and open symbols, respectively). Note that HERAGN represents a transition population, consistent with "green valley" objects, while LERAGN predominantly occupies the red sequence.

V.S. thanks Amy Kimball for help with the Unified Radio Catalog, as well as Nick Scoville and Scott Schnee for insightful comments on this manuscript, and Dominik A. Riechers for help with choosing "proper" colors in the last figure. The National Radio Astronomy Observatory is a facility of the National Science Foundation operated under cooperative agreement by Associated Universities, Inc.

REFERENCES

Allen, S. W., Dunn, R. J. H., Fabian, A. C., Taylor, G. B., & Reynolds, C. S. 2006, MNRAS, 372, 21
Baldwin, J. A., Phillips, M. M., & Terlevich, R. 1981, PASP, 93, 5
Bell, E. F., et al. 2004a, ApJ, 608, 752
Bell, E. F., et al. 2004b, ApJ, 600, L11
Best, P. N., Kaiser, C. R., Heckman, T. M., & Kauffmann, G. 2006, MNRAS, 368, L67
Best, P. N., Kauffmann, G., Heckman, T. M., & Ivezić, Ž. 2005, MNRAS, 362, 9
Borch, A., et al. 2006, A&A, 453, 869
Bower, R. G., Benson, A. J., Malbon, R., Helly, J. C., Frenk, C. S., Baugh, C. M., Cole, S., & Lacey, C. G. 2006, MNRAS, 370, 645
Brown, M. J. I., Dey, A., Jannuzi, B. T., Brand, K., Benson, A. J., Brodwin, M., Croton, D. J., & Eisenhardt, P. R. 2007, ApJ, 654, 858
Bundy, K., et al. 2008, ApJ, 681, 931

Buttiglione, S., Capetti, A., Celotti, A., Axon, D. J., Chiaberge, M., Macchetto, F. D., & Sparks, W. B. 2009, A&A, 495, 1033
Croton, D. J., et al. 2006, MNRAS, 365, 11
Evans, D. A., Worrall, D. M., Hardcastle, M. J., Kraft, R. P., & Birkinshaw, M. 2006, ApJ, 642, 96
Faber, S. M., et al. 2007, ApJ, 665, 265
Fanaroff, B. L., & Riley, J. M. 1974, MNRAS, 167, 31
Hardcastle, M. J., Evans, D. A., & Croston, J. H. 2006, MNRAS, 370, 1893
Heckman, T. M., Kauffmann, G., Brinchmann, J., Charlot, S., Tremonti, C., & White, S. D. M. 2004, ApJ, 613, 109
Ho, L. C. 2005, Ap&SS, 300, 219
Hopkins, P. F., Bundy, K., Hernquist, L., & Ellis, R. S. 2007, ApJ, 659, 976
Hopkins, P. F., et al. 2006, ApJS, 163, 1
Kauffmann, G., Heckman, T. M., & Best, P. N. 2008, MNRAS, 384, 953
Kauffmann, G., et al. 2003a, MNRAS, 341, 33
Kauffmann, G., et al. 2003b, MNRAS, 346, 1055
Kewley, L. J., Dopita, M. A., Sutherland, R. S., Heisler, C. A., & Trevena, J. 2001, ApJ, 556, 121
Kewley, L. J., Groves, B., Kauffmann, G., & Heckman, T. 2006, MNRAS, 372, 961
Kimball, A. E., & Ivezić, Ž. 2008, AJ, 136, 684
Ledlow, M. J., & Owen, F. N. 1996, AJ, 112, 9
Nesvadba, N. P. H., Lehnert, M. D., De Breuck, C., Gilbert, A. M., & van Breugel, W. 2008, A&A, 491, 407
Schinnerer, E., et al. 2007, ApJS, 172, 46
Sijacki, D., & Springel, V. 2006, MNRAS, 366, 397
Sijacki, D., Springel, V., di Matteo, T., & Hernquist, L. 2007, MNRAS, 380, 877
Smolčić, V., et al. 2006, MNRAS, 371, 121
Smolčić, V., et al. 2008, ApJS, 177, 14
Smolčić, V., et al. 2009, ApJ, 696, 24
Tremaine, S., et al. 2002, ApJ, 574, 740
White, S. D. M., & Frenk, C. S. 1991, ApJ, 379, 52
White, S. D. M., & Rees, M. J. 1978, MNRAS, 183, 341
Willott, C. J., Rawlings, S., Blundell, K. M., Lacy, M., & Eales, S. A. 2001, MNRAS, 322, 536